Mon. Not. R. Astron. Soc. **000**, 000–000 (0000) Printed 19 September 2012 (MN LATEX style file v2.2)

A Re-examination of Galactic Conformity and a Comparison with Semi-analytic Models of Galaxy Formation

Guinevere Kauffmann[1⋆], Cheng Li[2], Wei Zhang[3], Simone Weinmann[4]
[1]*Max-Planck Institut für Astrophysik, 85741 Garching, Germany*
[2]*Max-Planck-Institut Partner Group, Shanghai Astronomical Observatory, China*
[3]*National Astronomical Observatories, Chinese Academy of Sciences, Beijing 100012, China*
[4]*Leiden Observatory, P.O.Box 9513, 2300 RA Leiden, The Netherlands*

19 September 2012

ABSTRACT

The observed correlation between star-formation in central galaxies and in their neighbours (a phenomenon dubbed "galactic conformity") is in need of a convincing physical explanation. To gain further insight, we use a volume-limited sample of galaxies with redshifts less than 0.03 drawn from the SDSS Data Release 7 to investigate the scale dependence of the effect and how it changes as a function of the mass of the central galaxy. Conformity extends over a central galaxy stellar mass range spanning two orders of magnitude. The scale dependence and the precise nature of the effect depend on the mass of the central. In central galaxies with masses less than $10^{10}M_{\odot}$, conformity extends out to scales in excess of 4 Mpc, well beyond the virial radii of their dark matter halos. For low mass central galaxies, conformity with neighbours on very large scales is only seen when they have low star formation rate or gas content. In contrast, at high stellar masses, conformity with neighbours applies in the gas-rich regime and is clearly confined to scales comparable to the virial radius of the dark matter halo of the central galaxy. Our analysis of a mock catalogue from the Guo et al (2011) semi-analytic models shows that conformity-like effects arise because gas-poor satellite galaxies are sometimes misclassified as centrals. However, the effects in the models are much weaker than observed. Mis-classification only influences the low-end *tail* of the SFR/M_* distribution of neighbouring galaxies at large distances from the primary. The median and the upper percentiles of the SFR/M_* distribution remain almost unchanged, which is in contradiction with the data. We speculate that the conformity between low-mass, gas-poor central galaxies and their distant neighbours may be a signature of "pre-heating" of the intergalactic gas at an earlier epoch. The smaller-scale conformity between high-mass, gas-rich central galaxies and their close neighbours may be a signature of ongoing gas accretion onto central galaxies in a minority of massive dark matter halos.

Key words: galaxies: evolution – galaxies: haloes – galaxies:statistics

1 INTRODUCTION

In a system of orbiting galaxies, the largest and most massive galaxy is often referred to as the "primary", and the others are called satellites. The relationship between satellite galaxies and their primaries is one of the key tests of hierarchical galaxy formation models. In such models, galaxies form as cools and condenses at the centers of dark matter halos. As time progresses, dark matter halos merge and this leads to the formation of systems of galaxies orbiting within a common potential well. With the advent of large, wide-field imaging and spectroscopic surveys, there have been numerous studies of the properties satellite galaxies (e.g. McKay et al 2002; Prada et al 2003; Sales & Lambas 2004; Berlind et al 2005; Yang et al 2005; Weinmann et al 2006; Yang et al 2008; Norberg et al 2008; More et al 2009)

The behaviour of the average line-of-sight velocity dispersion of satellites as a function of distance from the primary galaxy, as well as the number density distribution of satellites as a function of projected radius, probes the den-

⋆ E-mail: gamk@mpa-garching.mpg.de

sity distribution of dark matter in galactic halos. In general, the velocity dispersion distributions and density profiles satellites galaxies are in reasonably good agreement with the predictions of the ΛCDM model (Prada et al 2003; Guo et al 2011). In recent work, Wang & White (2012) and Sales et al (2012) have shown that the luminosity and stellar mass functions of satellite galaxies predicted by semi-analytic models of galaxy formation embedded within high resolution cosmological N-body simulations agree well with results derived from the Sloan Digital Sky Survey.

Our understanding of the observed colours, star formation rates and gas content of satellites is still not complete. These properties are extremely sensitive to the physical processes that regulate how gas is supplied to these systems. In addition, both hydrodynamical and gravitational forces act to remove gas from satellites. Galaxy formation models developed in the 1990's (e.g. Kauffmann et al 1993, Cole et al 1994) generally assumed that the diffuse gas halos surrounding galaxies were stripped instantaneously as soon as they became satellites. There is then no further supply of new gas to satellites, and they redden with respect to the primary galaxy as their internal reservoir of cold gas is consumed. Subsequent work found that these models predicted satellites that were too red to be consistent with observations (Weinmann et al 2006; Baldry et al 2006). Current models attempt to model tidal and ram-pressure stripping of the diffuse gas in a more realistic way (Font et al 2008; Weinmann et al 2010; Guo et al 2011) and they produce satellite colour distributions in better agreement with the data.

We note that gas removal processes such as tidal interactions and ram-pressure stripping operate predominantly on smaller satellite galaxies, leaving the interstellar medium of the primary galaxy unperturbed. Only in the case of a very close encounter, would star formation in the primary galaxy respond to the presence of a satellite. The discovery that the properties of satellite galaxies are strongly correlated with those of their central galaxy, a phenomenon that has been called "galactic conformity" (Weinmann et al 2006), thus remains something of an enigma.

Yang et al (2006) suggest that a halo that assembled a significant fraction of its mass at an early epoch, may have accreted all its satellites at higher redshifts than a similar halo that assembled late. They proposed that galactic conformity may thus be a straightforward manifestation of hierarchical structure formation and thus ought to be detectable in galaxy catalogues generated from N-body simulations + semi-analytic models. Wang & White (2012) analyzed mock galaxy catalogues generated from the semi-analytic models of Guo et al (2011). These authors find a conformity effect in the models and show that it arises because red central galaxies inhabit more massive dark matter halos than blue galaxies of the same stellar mass.

Other authors have argued that more exotic hydrodynamical effects may be at play. Ann, Park & Choi(2008) argue that feedback processes that operated as the central galaxy formed affected the ability of surrounding galaxies to form stars. Kauffmann, Li & Heckman (2010) suggest that conformity is related to gas accretion. They propose that gas-rich satellites trace an underlying reservoir of ionized gas that is extended over large spatial scales, and that this reservoir fuels star formation in both the satellites and in the primary.

In an attempt to determine which viewpoint is correct, we have undertaken a re-analysis of galactic conformity using both Sloan Digital Sky Survey data and the publically available galaxy catalogues of Guo et al (2011). We have made the following changes to the analysis procedures that were employed in previous papers:

(i) We restrict the analysis to a volume-limited sample of galaxies from the spectroscopic catalogue with $\log M_* > 9.25$ and with redshifts in the range $0.017 < z < 0.03$. Previous analyses of satellites have made use of much fainter galaxies identified in the SDSS imaging data without spectroscopic redshifts. It has thus been necessary to account for contamination from galaxies physically unrelated to the primary by means of statistical background subtraction. Our restriction to a sample of very nearby galaxies with spectroscopic redshifts decreases the number of primary galaxies we are able to analyze by large factor, but it produces a much "purer" set of satellites. The quantitative comparison with semi-analytic models is also greatly simplified.

(ii) Because we are not limited by background subtraction errors, we are able to analyze conformity effects out to projected radii of 4-5 Mpc. The analysis of Kauffmann, Li & Heckman (2010) showed that correlations between satellite and central properties were still clearly present at projected separations of $\sim$ 1 Mpc. The analysis of Wang & White (2012), was restricted to satellites within a projected distance of 300 kpc from the primary galaxy, so did not address the question of whether conformity persists out to large physical scales. In addition, we are now able to analyze the *full distribution function of specific star formation rates* in the population of neighbouring galaxies. It is very difficult to do this accurately using photometric data.

(iii) Previous work has focused only on average colours, star formation rates and inferred gas fractions of satellite galaxies. In this analysis, we look at how *relations* between star formation rate, stellar mass and structural parameters change for galaxies located in the vicinity of red and blue primaries.

In agreement with previous results, we find conformity between the properties of central galaxies and their neighbours over a central galaxy stellar mass range spanning two orders of magnitude. However, our new analysis shows that the scale dependence of the effect depends on the mass of the central. Conformity effects extend to scales in excess of 4 Mpc around low mass central galaxies and the strongest effects are seen at large separations ($>$ 1 Mpc) from the primary. In contrast, for high mass central galaxies, conformity is clearly confined to scales less than 1-2 Mpc (i.e. within the scale of the dark matter halo). Conformity is only seen for low mass central galaxies when they have lower-than-average star formation rate or gas content. Conformity applies when high mass central galaxies are gas-rich and strongly star-forming. The observational results are not well-reproduced by the current Guo et al (2011) semi-analytic models.

Our paper is organized as follows. In section 2, we describe the data used in this analysis. In section 3, we present results from the SDSS DR7 spectroscopic sample. These results are compared with the Guo et al. models in section 4. In sections 5 and 6, we summarize and discuss possible implications of our findings. Throughout this paper, we as-

sume a spatially flat concordance cosmology with $\Omega_m = 0.3$, $\Omega_\Lambda = 0.7$, and $H_0 = 70$ km s^{-1}Mpc^{-1}.

2 ANALYSIS TOOLS

2.1 Data

We begin with the parent galaxy sample constructed from the New York University Value Added Catalogue (NYU-VAGC) sample dr72 (Blanton et al. 2005), which consists of about half a million galaxies with $r < 17.6$, $-24 < M_r < -16$ and redshifts in the range $0.01 < z < 0.5$. Here, r is the r-band Petrosian apparent magnitude, corrected for Galactic extinction, and M_r is the r-band Petrosian absolute magnitude, corrected for evolution and K-corrected to its value at $z = 0.1$.

From the parent sample, we select a volume-limited sample of galaxies with $\log M_* > 9.25$ and redshifts in the range $0.017 < z < 0.03$. The lower limit in redshift ensures that we do not consider galaxies where the peculiar velocity would affect the conversion from redshift into distance by a significant factor. The upper limit in redshift ensures that we are able to detect all galaxies down to a limiting stellar mass of $2 \times 10^9 M_\odot$, irrespective of the intrinsic colour of the system. These cuts result in a sample of 11,673 galaxies.

We define a galaxy with mass M_* to be a central galaxy if there is no other galaxy with with stellar mass greater than $M_*/2$ within a projected radius of 500 kpc and with velocity difference less than 500 km s^{-1}. There are 7712 galaxies in our catalogue with stellar masses greater than $5 \times 10^9 M_\odot$ to which we can apply this criterion; 4636 (i.e. 60%) are classified as central galaxies. As we will show, this is in reasonably good agreement with the predictions of the semi-analytic models of Guo et al (2011).

In this paper, we will make use of two different measures of gas content/star formation activity.

(i) The "pseudo" HI gas mass fraction estimates of Li et al (2012) utilize a combination of four galaxy parameters:

$$\begin{aligned}\log(M_{\rm HI}/M_*) &= -0.325 \log \mu_* - 0.237(NUV - r) \\ &\quad -0.354 \log M_* - 0.513\Delta_{g-i} + 6.504, \quad (1)\end{aligned}$$

where M_* is the stellar mass; μ_* is the surface stellar mass density given by $\log \mu_* = \log M_* - \log(2\pi R_{50}^2)$ (R_{50} is the radius enclosing half the total z-band Petrosian flux and is in units of kpc). $NUV - r$ is the global near-ultraviolet (NUV) to r-band colour. The NUV magnitude is provided by the GALEX pipeline and the $NUV - r$ colour is corrected for Galactic extinction following Wyder et al (2007) with $A_{NUV-r} = 1.9807 A_r$, where A_r is the extinction in the r-band derived from the dust maps of Schlegel, Finkbeiner & Davis (1998). Δ_{g-i} is the colour gradient defined as the difference in $g-i$ colour between the outer and inner regions of the galaxy. The inner region is defined to be the region within R_{50} and the outer region is the region between R_{50} and R_{90}. As discussed in Li et al (2012), the estimator has been calibrated using samples of nearby galaxies ($0.025 < z < 0.05$) with HI line detections from the GALEX Arecibo SDSS Survey (Catinella et al 2010).

(ii) The specific star formation rate (SFR/M_*) evaluated within the SDSS fibre aperture is estimated using the methodology described in Brinchmann et al (2004). These estimates are publically available for all galaxies in the DR7 galaxy sample at http://www.mpa-garching.mpg.de/SDSS/DR7/.

We note that the main difference between the two measures is that the first is mainly sensitive to the age of stars in the outer regions of the galaxy, while the second is sensitive to the amount of ongoing star formation in the core of the galaxy (At the median redshift of the galaxies in our sample, the 3 arcsecond diameter SDSS fibre subtends a physical scale of only 1.37 kpc).

2.2 Models

In this paper we compare our observational results to predictions from the galaxy formation models of Guo et al (2011; hereafter G11) This model was created by implementing prescriptions for baryonic astrophysics on merger trees that follow the evolution of the halo/subhalo population in the Millennium-II (MSII; Boylan-Kolchin et al. 2009) Simulation, a cubic region 137 Mpc on a side containing 2160^3 particles with mass $9.45 \times 10^6 M_\odot$. The G11 model is the most recent semi-analytic model from the Munich group, in which the treatments of many of the physical processes have been significantly updated. G11 demonstrated that their model provided good fits not only to the luminosity and stellar mass functions of galaxies derived from SDSS data, but also to recent determinations of the abundance of satellite galaxies around the Milky Way and the clustering properties of galaxies as a function of stellar mass.

In this paper, we work with 13,830 galaxies with stellar masses greater than $2 \times 10^9 M_\odot$ from the $z = 0$ output of the simulation. We identify central galaxies in the simulation box in the same way as in the observations, but in the simulation we know which galaxies are true central and satellite systems, so this allows us to evaluate the efficacy of our procedure. In the left-hand panel of Figure 1, the thick dashed line shows the fraction of satellite galaxies F(sat) as a function of stellar mass for the simulated galaxies; it decreases from 0.55 at $M_* = 3 \times 10^9 M_\odot$ to around 0.25 at $M_* = 3 \times 10^{11} M_\odot$. The thin lines show F(sat) once the isolation cuts have been applied. Red, black, green, blue and cyan lines are for galaxies with increasing cold gas fractions. At the low mass end, the isolation cuts decrease F(sat) by a factor of between 2 and 5, depending on gas fraction. At the high mass end, the cuts have much smaller effect. This is because the relation between central galaxy and dark matter halo mass is rather flat for high mass halos and as a result, the true central galaxy is not always the most massive galaxy in its immediate environment. Nevertheless, we see that the predicted contamination from satellites is always below 30% for galaxies of all stellar masses and gas fractions.

3 RESULTS FROM SDSS

3.1 Dependence of conformity on the stellar mass of the primary, separation of the neighbour, and star formation activity tracer

In this section, we carry out a systematic exploration of how conformity between central galaxies and the surrounding population of neighbours depends on, a) the stellar mass

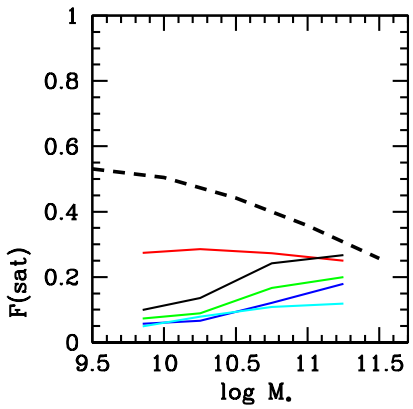

Figure 1. The thick dashed line shows the fraction of satellite galaxies as a function of stellar mass for all galaxies in the $z = 0$ Millennium II simulation output. The coloured lines show the fraction of satellites once we apply the same isolation criterion used to construct our SDSS central galaxy sample (see text for details). Red, black, green, blue and cyan curves are for simulated galaxies with cold gas mass fractions in the 0-25th percentile, 25-50th percentile, 50-75th percentile, $>$ 75th percentile and $>$ 90th percentile ranges of the full distribution.

of the central, b) the physical separation between the neighbour and the central, c) the indicators used to trace star formation and cold gas content in both the centrals and in their neighbours.

Figures 1-4 in this section focus on how the specific star formation rates and gas content of the neighbouring galaxy population vary as a function of projected radius from the central. Figures 5-6 then explore how the *relations* between specific star formation rate/gas content and galaxy mass/structural parameters for neighbouring galaxies change according to the properties of the central object.

We begin with the subset of central galaxies with stellar masses in the range $10.0 < \log M_* < 10.5$. We divide these galaxies into quartiles using four different measures:

(i) The "pseudo" HI mass fraction estimate given in equation 1. Hereafter, we will denote this quantity as GS(M_*).

(ii) The "HI deficiency parameter" defined in Li et al. (2012), which is the deviation in $\log(M_{HI}/M_*)$ from the value predicted from the mean relation between $\log(M_{HI}/M_*)$ and the combination of galaxy mass M_* and stellar surface mass density μ_* . Li et al (2012) showed that the amplitude of the correlation function on scales of 1-2 Mpc varied much more strongly as a function of the HI deficiency parameter than as a function of the "pseudo" HI mass fraction. In subsequent work, Zhang et al (2012) found that depletion of gas in galaxies in groups and clusters depended more strongly on the stellar surface density of the galaxy than on the mass of the galaxy. It is thus instructive to fix *both stellar mass and galaxy size* when we investigate how galaxies are affected by their environment.

(iii) The specific star formation rate SFR/M_* evaluated within the 3 arcsecond diameter fibre aperture. As we have discussed, this quantity should be regarded as a measure of recent star formation activity in the central regions of the galaxy.

(iv) The total specific star formation rate. We note that our estimate of SFR(total) is dominated by the aperture correction to SFR(fibre). In Brinchmann et al (2004), which was based on SDSS DR4 data, the aperture corrections were done in an empirical manner. The procedure was later found to over-estimate the SFR of red galaxies (Salim et al 2007). In the DR7 release, the aperture corrections are computed by fitting the SDSS 5-band photometry of the outer galaxy to a library of spectral energy distributions generated using population synthesis models.

In Figure 2, results for galaxies in four quartiles of HI gas mass fraction, HI deficiency parameter, fibre and total specific SFR/M_* are shown as red, black, green and blue curves, respectively. The cyan curves show results for galaxies in the upper 90th percentiles of these quantities, i.e. cyan curves are for very unusually gas-rich or strongly star-forming central galaxies. The solid curves show the median fibre-based specific star formation rate of neighbouring galaxies as a function of projected distance (in Mpc) from the central object. The lower and upper set of dotted lines show the 25th and 75th percentiles this quantity.

Fow all central galaxy bins, the specific star formation rates of neighbours as a function of projected radius first exhibit a drop, and then flatten out at radii larger than 500 kpc. This scale is artificially *imposed* by our definition that a central galaxy has to be a factor of two more massive than any neighbour within a projected radius of 500 kpc. Low mass galaxies have higher specific star formation rates than high mass galaxies, so by eliminating any galaxies with massive companions within $R_{proj} = 500$ kpc, the specific star formation rates are forced to change in a discontinuous way at this radius.

It is apparent that for central galaxies with stellar masses $\sim 10^{10} M_\odot$, conformity between central galaxies and neighbours is strong if the centrals have gas mass fractions/specific star formation rates less than the median value. It is absent for central galaxies with gas fractions and SFR/M_* values higher than the median. It is also apparent that conformity extends out to very large projected separations. In all four panels, the black curve does not converge to meet the cyan, blue and green curves until a projected radius of $R = 3$ Mpc. The red curve, which shows results for the 25% most gas-poor/weakly star-forming galaxies, remains depressed out beyond $R = 4$ Mpc. These are scales well beyond the virial radius of a $10^{10} M_\odot$ galaxy! These conclusions are independent of the choice of star formation activity indicator. Finally, conformity is most pronounced when the central galaxies are ordered by global HI deficiency and total specific star formation rate, rather than central SFR/M_*.

Figure 3 is the same as Figure 2, except that results are shown for central galaxies with stellar masses in the range $10^{11} - 3 \times 10^{11} M_\odot$. There are many fewer galaxies in this stellar mass bin, so the errorbars are larger, but it is nevertheless clear that the results are strikingly different. First, conformity effects are only apparent for galaxies in the upper quartile of HI gas mass fraction, HI deficiency and total specific star formation rate. Second, unlike Figure 2, no conformity is seen if the central galaxies are ordered by central specific star formation rate. Third, conformity is largest at

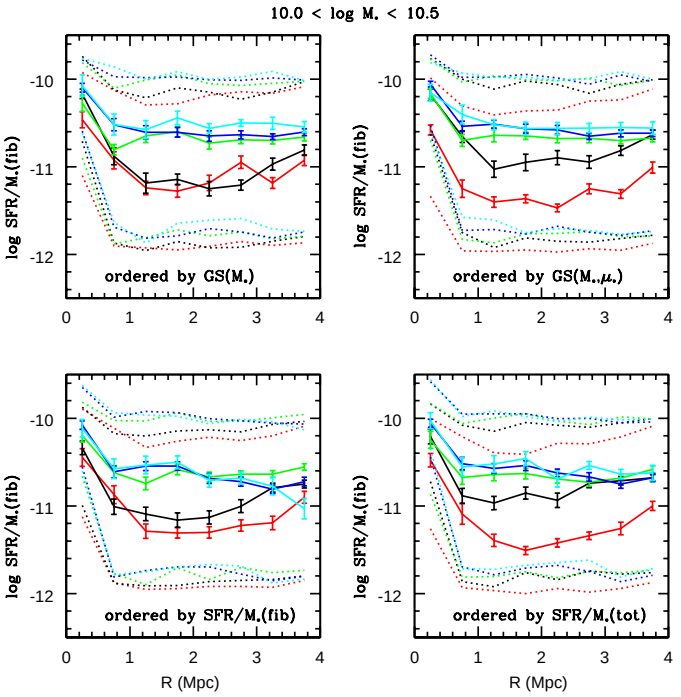

Figure 2. The specific star formation rate (measured within the SDSS fibre aperture) of neighbouring galaxies is plotted as a function of projected distance from the central galaxies. Results are shown for central galaxies in the stellar mass range $10 < \log M_* < 10.5 M_\odot$. In each of the four panels, the central galaxies have been ordered by a different quantity: a) "pseudo" HI mass fraction (top left), b) HI deficiency parameter (top right), c) fibre specific star formation rate (bottom left), d) total specific star formation rate (bottom right). Red, black, green, blue and cyan curves indicate results for central galaxies that fall into the 0-25th percentile, 25-50th percentile, 50-75th percentile, $>$ 75th percentile and $>$ 90th percentile ranges of distribution of these four quantities. Solid curves indicate the median of the SFR/M_* distribution for neighbouring galaxies at given radius, while upper and lower dotted curves indicate the 25th and 75th percentiles of the SFR/M_* distribution. Errorbars on the median have been computed via boot-strap resampling.

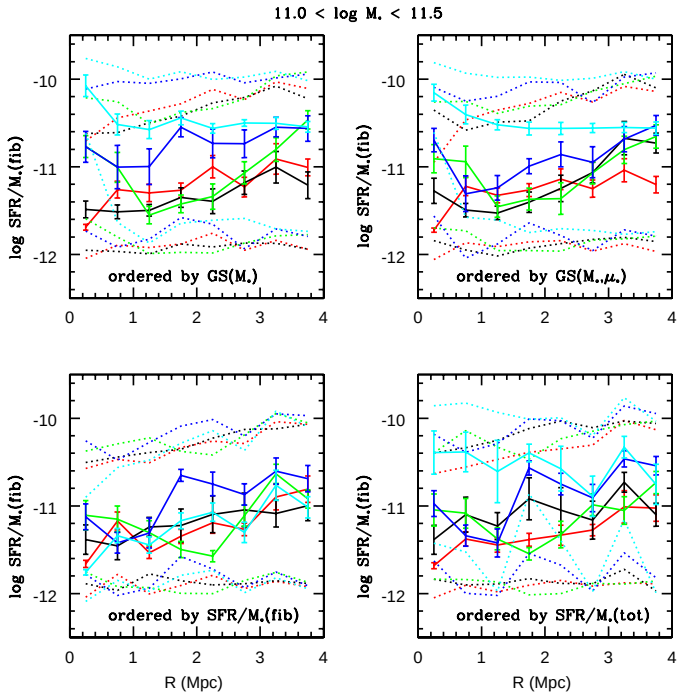

Figure 3. As in Figure 2, except for central galaxies in the stellar mass range $11 < \log M_* < 11.5 M_\odot$.

small separations and disappear at projected radii beyond $\sim 2-3$ Mpc.

In Figure 4, we investigate trends with stellar mass in more detail by showing results in four different central galaxy stellar mass bins spanning the range $M_* = 5\times10^9 M_\odot$ to $3\times10^{11} M_\odot$. For simplicity, we only show the case where the central galaxies are ordered by HI deficiency. At low stellar masses, conformity is strongest on large scales and applies only in the gas-poor regime. At high stellar masses, conformity is strongest on small scales and applies only in the gas-rich regime. The cross-over between the two regimes occurs for central galaxies with stellar masses $\sim 3\times10^{10} M_\odot$. In the $10.5 < \log M_* < 11 M_\odot$ bin, conformity is seen both on small scales for gas-rich central galaxies, and on large scales for gas-poor central galaxies.

So far, we have only investigated the sensitivity of conformity to the indicator used to partition central galaxies into gas-rich/strongly-star-forming and gas-poor/weakly-star-forming systems. We concluded that conformity is

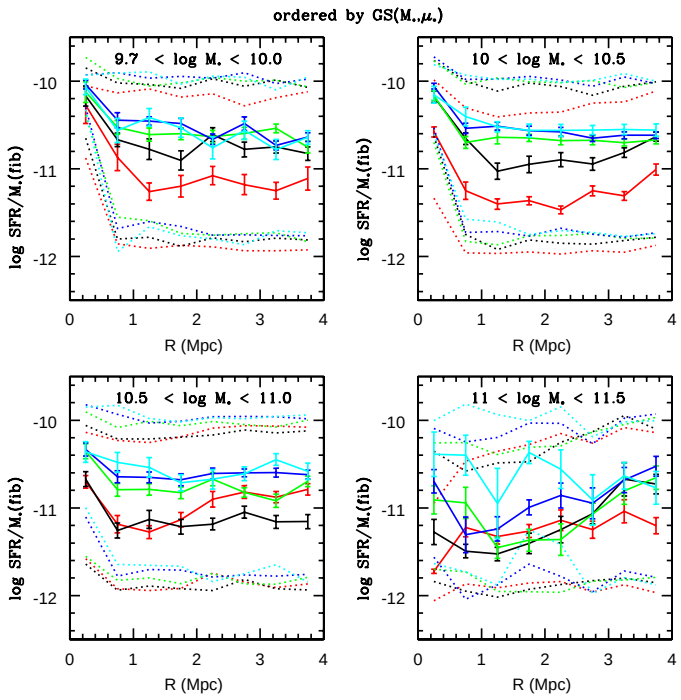

Figure 4. As in Figure 2, except results are shown for central galaxies in four different stellar mass ranges. For simplicity, we only show the case where central galaxies are ordered by HI deficiency.

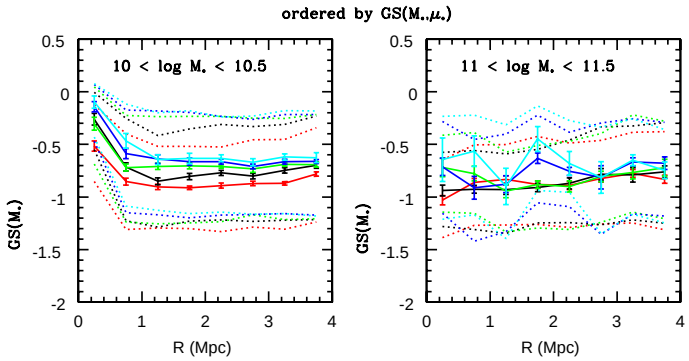

Figure 5. As in Figure 4, except results are shown for central galaxies in two different stellar mass ranges and we plot the pseudo gas fractions of their neighbours, rather than their fibre specific star formation rates.

strongest when the central galaxies are sorted according to global quantities (total gas content and total specific star formation rate). What about the neighbours? Figure 5 is the same as Figure 4, except that we plot the pseudo gas fractions of the neighbours instead of their central specific star formation rates. The amplitude of conformity effect is now much smaller. In the $10 < \log M_* < 10.5 M_\odot$ bin, the difference in the median SFR/M_*(fibre) for neighbours around the most gas-rich centrals compared the most gas-poor centrals is nearly a factor of 10. In contrast, the difference in the gas fraction is less than a factor of 2. This decrease in the amplitude holds in all four stellar mass bins.

What we conclude, therefore, is that an excess or deficiency in the gas content of central galaxies is most intrinsically correlated with the timescale over which their neighbours have been building their *central* stellar populations.

3.2 Correlations between different galaxy properties in neighbouring galaxies

In the previous section, we examined how the median specific star formation rates and gas fractions of neighbouring galaxies at a given projected radius correlated with the properties of the central object. In this section, we study changes in the *relations* between different satellite properties such as stellar mass, stellar surface density, concentration index, specific star formation rate and gas mass fraction.

As discussed in the previous subsection, conformity is strongest on large scales for low mass centrals, and on small scales for high mass centrals. Here we analyze central galaxies in two different stellar mass ranges: $9.7 < \log M_* < 10.3 M_\odot$ and $10.7 < \log M_* < 11.5 M_\odot$. For the lower mass bin, we pick all neighbours with projected radii between 1 and 3 Mpc and $\Delta cz < 500$ km/s and we plot relations between different properties in Figure 6. For central galaxies in the higher mass bin, we pick satellites with projected radii less than 0.6 Mpc and plot the corresponding relations in Figure 7. In both plots, red, black, green and blue curves denote median relations for neighbours around central galaxies divided into four quartiles in HI deficiency parameter.

Echoing results presented in the previous section, we see that conformity effects only apply in the low-gas fraction regime for low mass central galaxies (i.e. the blue and

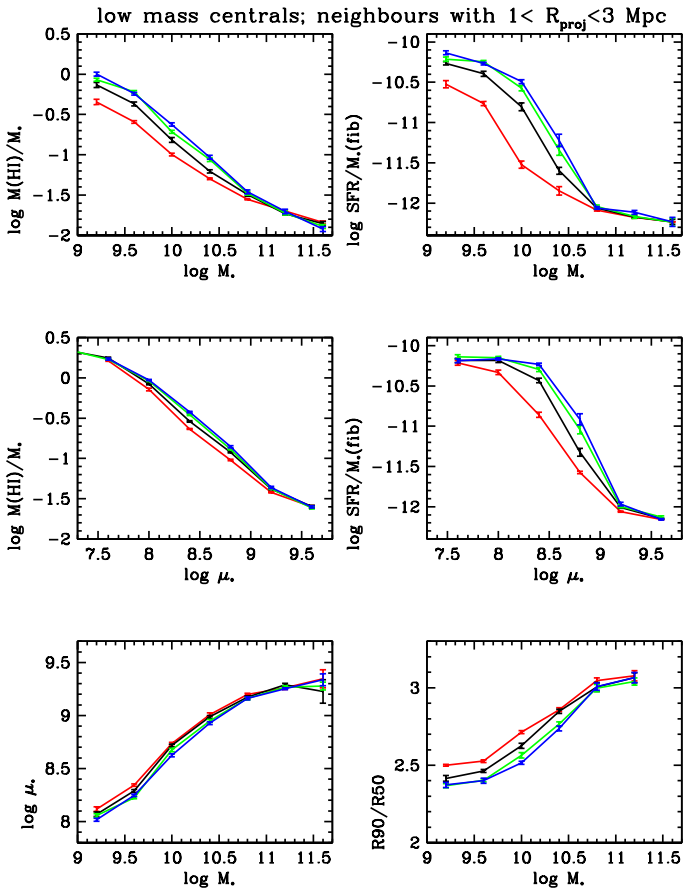

Figure 6. The relations between pseudo gas mass fraction and stellar mass (top left), fibre specific star formation rate and stellar mass (top right), pseudo gas mass fraction and stellar surface mass density (middle left), fibre specific star formation rate and stellar surface mass density (middle right), stellar surface mass density and stellar mass (bottom left) and concentration and stellar mass (bottom right), for distant neighbours of central galaxies with stellar masses in the range $9.7 < \log M_* < 10.3$. Distant neighbours are defined to be at projected radii between 1 and 3 Mpc from the central galaxy and to have velocity difference $\Delta(cz) < 500$ km/s. Red, black, green, blue and cyan curves are for central galaxies with HI deficiency parameters in the 0-25th percentile, 25-50th percentile, 50-75th percentile and > 75th percentile ranges of the full distribution.

green curves are almost indistinguishable in Figure 6). For high mass central galaxies, conformity effects extend into the high gas mass fraction regime. In both Figures 6 and 7, we see that the largest changes occur in the relations between specific star formation rate measured in the fibre and galaxy mass and stellar surface density. Relations between structural parameters such as concentration and stellar surface density and stellar mass change more weakly. The largest changes in specific star formation rate occur for neighbours with stellar masses below a few $\times 10^{10} M_\odot$ and with stellar surface mass densities of a few $\times 10^8 M_\odot$ kpc^{-2}. In this regime, the median value of SFR/M_* changes from values around 1/15. Gyr^{-1} for neighbours around gas-rich central galaxies, to values around 1/100 Gyr^{-1} for neigh-

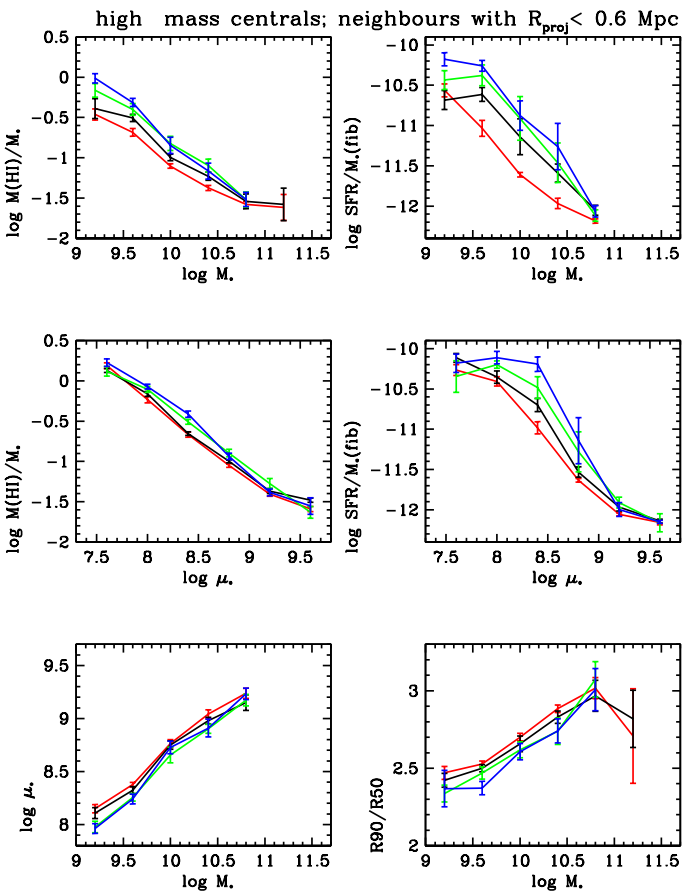

Figure 7. As in Figure 6, except for near neighbours of central galaxies with stellar masses in the range $10.7 < \log M_* < 11.5$. Near neighbours are defined to be at projected radii less than 600 kpc from the central galaxy and to have velocity difference $\Delta(cz) < 500$ km/s.

bours around gas-poor central galaxies. In other words, if such a neighbour is found around a gas-rich central, it is building up its central stellar mass over timescales comparable to the Hubble time. If it is found around a gas-poor central, the growth time of the central region of the galaxy is an order-of-magnitude longer. It is also interesting that the galaxy parameter regime where conformity effects are strongest is the same as the parameter regime of host galaxies of actively accreting present-day black holes (Heckman et al 2004).

Finally, Figure 8 is a simple summary of what we believe to be the main result of this section. We compare the systematic changes in the relations between fibre specific star formation rate and stellar surface mass density for distant neighbours around low mass centrals (left) with those for near neighbours around high mass centrals (right). Note that we have added central galaxies in the upper 90th percentile in HI content as a cyan curve in each panel. The difference in behaviour in the two panels as a function of the gas content of the central galaxies is quite striking. We will discuss possible interpretations in the final section.

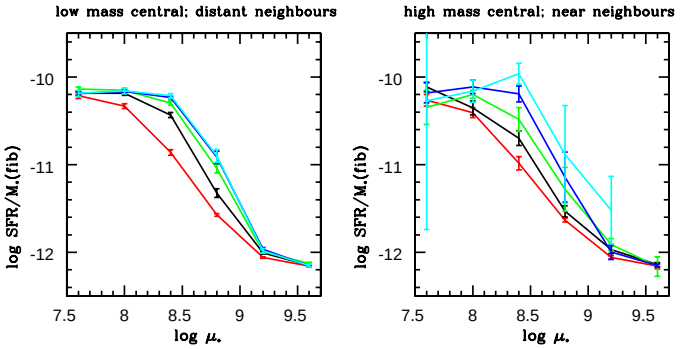

Figure 8. The relations between fibre specific star formation rate and stellar surface mass density for distant neighbours of central galaxies with stellar masses in the range $9.7 < \log M_* < 10.3$ (left) and for close neighbours of central galaxies with stellar masses in the range $10.7 < \log M_* < 11.3$ (right). Red, black, green, blue and cyan curves are for central galaxies with HI deficiency parameters in the 0-25th percentile, 25-50th percentile, 50-75th percentile, > 75th percentile and > 90th percentile ranges of HI deficiency parameter.

4 RESULTS FROM SEMI-ANALYTIC MODELS

In this section, we present results from the semi-analytic model galaxy catalogues. As discussed in the introduction, Wang & White (2012) have analyzed conformity in these models and claim that the observed trends are explained because red galaxies inhabit more massive halos than blue galaxies of the same mass. We do not disagree with the statement that the halo masses of red and blue galaxies of the same M_* are different . As seen in Figure 1, the fraction of central galaxies that are mis-classified even after our isolation criterion is applied is significantly higher for gas-poor galaxies – all of these mis-classified centrals are satellite systems in massive halos. However, as we will show in this section, *this effect cannot explain the trends seen in the observations.*

The Guo et al (2011) model does not include detailed modelling of the density profiles of the stars and gas, so we only work with global specific star formation rates and gas fractions in this section. Figure 9 is analogous to Figure 2: we plot the specific star formation rates of neighbours as a function of projected distance from central galaxies with stellar masses in the range $10 < \log M_* < 10.5 M_\odot$. As in the previous section, we partition the central galaxies into quartiles in gas mass fraction (left) and global specific star formation rate (right). Solid curves show the median value of $\log SFR/M_*$ for the satellites as a function of projected radius, while the lower and upper dotted curves show the 25th and 75th percentiles of the distributions. As in previous plots, red, black, green, blue and cyan curves colour-code results for central galaxies with increasing gas fraction and SFR/M_*.

Similar to what is found in the observations, conformity mainly applies in the low gas fraction/ specific star formation rate regime. However, in the data, the *median* specific star formation rate of the neighbours shifts by a factor of $5 - 10$ between gas-poor and gas-rich central galaxies and the upper 75th perctiles of the distribution also show a pronounced effect. In the models, the median shifts by less than

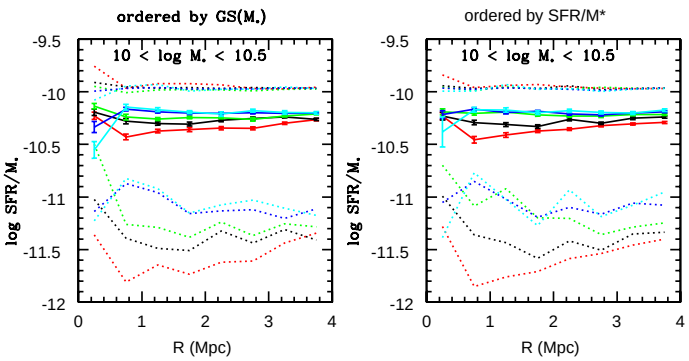

Figure 9. The specific star formation rate of neighbouring galaxies is plotted as a function of projected distance from central galaxies identified in galaxy catalogues generated using the Guo et al (2011) semi-analytic models. Results are shown for central galaxies in the stellar mass range $10 < \log M_* < 10.5$. The central galaxies have been ordered by cold gas mass fraction (left), and specific star formation rate (right). Red, black, green, blue and cyan curves indicate results for central galaxies that fall into the 0-25th percentile, 25-50th percentile, 50-75th percentile, $>$ 75th percentile and $>$ 90th percentile ranges of distribution of these four quantities. Solid curves indicate the median of the SFR/M_* distribution for neighbouring galaxies at a given radius, while upper and lower dotted curves indicate the 25th and 75th percentiles of the SFR/M_* distribution.

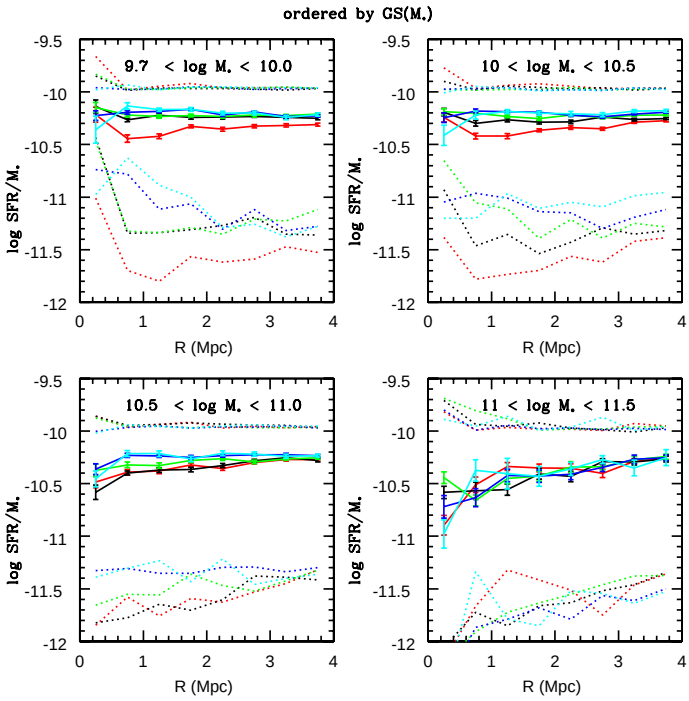

Figure 10. The specific star formation rate of neighbouring galaxies is plotted as a function of projected distance from central galaxies in the model. Results are shown for central galaxies in four stellar mass ranges. The central galaxies have been ordered by cold gas mass fraction.

50% and the upper 75th percentile shows no effect whatsoever; the main shift is in the low SFR/M_* tail of the distribution. This is because conformity effects in the models are caused by the increasing fraction of true satellite galaxies among objects classified as centrals using our isolation criterion. However, Figure 1 shows that these mis-classifications never come to dominate the statistics, even in the case of the most gas-poor objects.

In Figure 10, we show model results for central galaxies in the same four bins of stellar mass as in Figure 4. The shifts in median SFR/M_* for neighbouring galaxies are very weak at all stellar masses. Stronger effects are seen for the lower 25th percentile of the distribution. Conformity also disappears completely at central galaxy stellar masses greater than $10^{11} M_\odot$, which again disagrees with the data.

Finally, the top two panels of Figure 11 show the relations between specific star formation rate and stellar mass for neighbours around low mass and high mass central galaxies. Once again, we see no shift in the median relation for neighbours around gas-rich and gas-poor central galaxies – only the lower percentiles of the distribution show a significant trend. These results disagree with those presented in Figures 6, 7 and 8.

So far we have established that there is very significant disagreement between the data and the models. Can we now use the simulations to gain insight into what has to be changed to obtain a better match to the observations? One question we might ask is whether we need to modify the physical processes regulating gas accretion and star formation in galaxies that reside at the centers of their dark matter halos, or whether it is the treatment of processes such as ram-pressure and tidal stripping in infalling satellites that needs changing, or both.

The middle panels of Figure 11 show the fraction of neighbouring galaxies that are *true satellites* in the simulation, i.e. the fraction that do not reside at the centers of their host dark matter halos. In the middle right panel, F(sat) is very close to unity, because we have only included galaxies in the close vicinity ($R < 600$ kpc) of massive centrals. The conformity between gas-rich massive galaxies and near neighbours seen in the right panel of Figure 8 could thus plausibly be recovered by suitable changes to the recipes for gas-stripping in the simulation.

In the left panel of Figure 11, we are considering neighbours out to much larger projected radii and F(sat) is around 0.5 on average. The fraction of true satellites among neighbours does depend on the gas fraction of the central object, but the effect is quite weak – F(sat) shifts by less than 50% between the most gas-rich and gas-poor central galaxies. Let us assume for argument's sake that all satellites are passive and have log SFR/$M_* \sim 10^{-12}$, and that all centrals are active with log SFR/$M_* \sim 10^{-10}$; a change in satellite fraction from 40% to 70% would only change the average in log SFR/M_* by 0.2 dex, which is far less than what is seen in Figure 6.

The bottom left panel shows the relation between halo mass and stellar mass for neighbouring galaxies around low mass centrals that are themselves central objects in their dark matter halos. In the models, this relation is quite insensitive to whether the low mass central is gas-rich or gas-poor. We therefore conclude that the conformity between gas-poor central galaxies with low stellar masses and distant neighbours requires quenching processes to be coor-

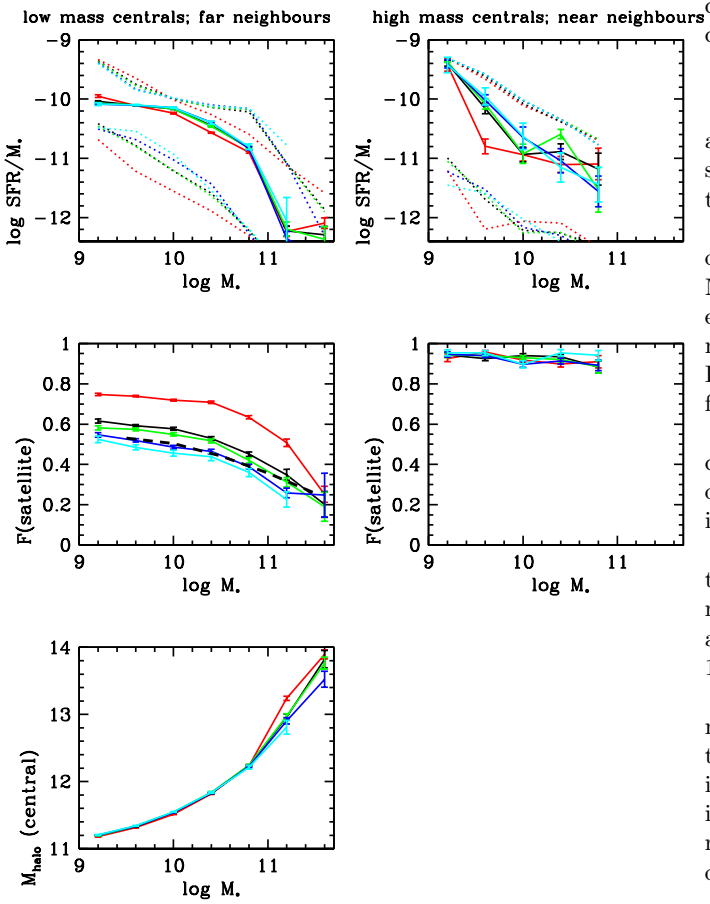

Figure 11. Top: For comparison with Figure 8, the relation between specific star formation rate and stellar mass is plotted for distant neighbours around low mass central galaxies (left) and for near neighbours around high mass central galaxies (right) in the models. Coloured lines indicate different ranges in central galaxy cold gas mass fraction, as before. **Middle:** The fraction of true satellite galaxies as a function of stellar mass in the distant neighbour population around low mass centrals (left); the same for the near neighbour population around high mass central (right). **Bottom left:** Dark matter halo mass is plotted against stellar mass for true central galaxies in the distant neighbour population around low mass centrals.

dinated in galaxies occupying *disjoint and widely-separated dark matter halos.*

5 SUMMARY

In this paper, we use a volume-limited sample of galaxies drawn from the SDSS Data Release 7 with stellar masses greater than $2 \times 10^9 M_\odot$ and redshifts less than 0.03 to perform a detailed analysis of the "conformity" between the star formation rates of central galaxies and those of neighbouring galaxies pointed out by Weinmann et al (2006). We investigate the scale dependence of the effect and how it changes as a function of the mass of the central. We also explore conformity a variety of different galaxy properties clarify which ones result in the strongest correlations between central galaxies their neighbours. Finally, we test whether current semi-analytic models are able to match the data.

Our main results are as follows:

- Conformity between the properties of central galaxies and their neighbours extends over the full central galaxy stellar mass range that we were able to explore ($5 \times 10^9 M_\odot$ to $3 \times 10^{11} M_\odot$).
- The scale dependence of the effect depends on the mass of the central. Conformity extends to scales in excess of 4 Mpc around low mass central galaxies and the strongest effects are seen at large separations (> 1 Mpc) from the primary, well beyond the virial radius of its dark matter halo. In contrast, for high mass galaxies, conformity is clearly confined to scales less than 1-2 Mpc.
- For low mass galaxies, conformity is only seen when the central galaxies have lower-than-average star formation rate or gas content. For high mass galaxies, conformity applies in the high gas fraction/specific star formation rate regime.
- The strongest conformity effects arise when gas in central galaxies is correlated with central specific star formation rates in neighbouring galaxies with stellar masses less than a few $\times 10^{10} M_\odot$ and stellar surface densities in the range $10^8 - 10^9 M_\odot$ kpc^{-2}.
- Conformity effects in the Guo et al (2011) models are much weaker than the ones that we observe. The effects in the models occur because a higher fraction of gas-poor galaxies are mis-classified as centrals, even after our isolation cut is applied. Matching the data for low mass central galaxies requires quenching processes to be coordinated in galaxies occupying disjoint and widely-separated dark matter halos.

6 DISCUSSION

In this section, we attempt to provide a physical interpretation of our results. We also speculate on why there is such strong disagreement between the models and the data. Finally, we discuss possible implications of our results for large-scale structure studies.

6.1 Low mass galaxies and "pre-heating".

Perhaps the most striking and puzzling new result presented in this paper is that conformity between low mass central galaxies and their neighbours extends over scales of many megaparsecs. Conformity applies to low mass centrals that have gas fractions lower than the median value, suggesting that "quenching" rather than accretion processes are at work.

Wang et al (2009) suggested that red, low mass central galaxies are actually satellites that have been "ejected" from massive halos after undergoing tidal and/or ram-pressure stripping. A full explanation of the conformity effect presented in this paper would require *more than half* of all low mass galaxies to have passed through a massive halo, which we deem to be unlikely. In addition, ejection of satellites would likely produce a disjoint population of red, low mass field galaxies around massive halos. As shown in the left panel of Figure 8, the median SFR/M_* of distant neighbours changes in a smooth way between the central galaxy

bins indicated by green, black and red curves. This is difficult to understand in the context of ejection.

An alternative possibility is that inter-galactic gas was heated over large spatial scales at some earlier epoch, preventing it from collapsing into halos, cooling and forming stars. In the literature, this has traditionally been referred to as "pre-heating". Pre-heating was originally proposed to explain why hydrodynamical simulations failed to reproduce the cluster temperature-X-ray luminosity relation (e.g. Valageas & Silk 1999). Implications of an early epoch of pre-heating on the present-day galaxy population were explored by Mo & Mao (2002). These authors postulated that vigorous energy feedback associated with star formation and AGN activity in galaxies at redshifts 2-3 would be responsible for the pre-heating. In subsequent work, Mo et al. (2005) explored the possibility that shocks produced as a consequence of gravitational collapse of large-scale structure could also heat the gas and prevent it from collapsing into halos. The predictions in this paper have not yet been verified using hydrodynamical simulations. The fact that conformity is only found for the neighbours of gas-poor galaxies with *low stellar masses* may point to energy sources that are internal rather than external to galaxies – supernovae and/or winds from accreting black holes will more easily reach the IGM if they are generated in low mass halos.

In the semi-analytic models, pre-heating of the IGM is modelled in a very rough way by placing some fraction of the gas in the halo into a so-called "ejected component" (De Lucia, Kauffmann & White 2004). This gas is not available for cooling until it is returned to the dark matter. In the Guo et al (2011) models, gas in the ejected component is returned to the halo in a few dynamical times for a Milky Way mass galaxy, but on longer timescales for lower mass galaxies. These models nevertheless overpredict the abundance of galaxies with stellar masses less than $\sim 10^{10} M_{\odot}$ at redshifts greater than ~ 0.6. Recent work has suggested that the problem of the overproduction of low mass galaxies at high redshifts is alleviated if the gas re-incorporation timescales are longer than assumed by Guo et al., particularly at higher redshifts (B. Henriques and S. White, private communication). It is unlikely that such models will do a better job of matching the observed conformity effects, because the ejected component is always returned to the same halo. If the ejected compoents of neighbouring galaxies were allowed to *mix*, it may be possible to obtain effects similar to those seen in the data.

6.2 High mass galaxies and accretion

Conformity between high mass central galaxies and their neighbours extends over spatial scales comparable to that of an individual massive dark matter halo. Conformity is strongest for a minority of the most gas-rich massive galaxies (see right panel of Figure 8), suggesting that accretion processes may be the underlying cause.

In Kauffmann, Li & Heckman (2010), it was argued that blue, star-forming satellites trace an underlying reservoir of ionized gas that provides fuel for ongoing star formation in central galaxies. Accretion of both dark matter and gas from the surrounding environment is modelled in detail in the semi-analytic models, so the question arises as to why similar conformity effects are not seen in the high stellar mass bins in Figure 10.

In the simulations, central galaxies with stellar masses of $\sim 10^{11} M_{\odot}$ reside in dark matter halos with masses of few $\times 10^{12} M_{\odot}$ (see bottom left panel of Figure 11). In the models, gas cooling in halos of this mass occurs from a corona of hot gas that is assumed to be in hydrostatic equilibrium with the surrounding dark matter halo. Cooling rates are regulated by "radio-mode feedback", with efficiency that scales with the black hole mass of the central galaxy multiplied by V_{vir}^3, where V_{vir} is the circular velocity of the dark matter halo (Croton et al 2006). Cooling rates are thus mainly determined by the mass of the halo in which the galaxy resides. Because the cooling equations *assume* that the gas is always in equilibrium with the dark matter, cooling rates are not sensitive to the dynamical state of the halo or to its satellite population.

One possibility is that massive galaxies surrounded by blue satellites reside in massive dark matter halos that have assembled relatively recently. Gas has not yet shocked and reached very high temperatures and is thus able to cool more efficiently onto the central object. The fact that the blue satellite population is most pronounced in the extreme tail of objects with the highest gas mass fractions, supports the notion that gas fuelling associated with blue satellites is a transient phase in the lives of these galaxies. Cooling and star formation may later be shut down by radio jets (see Chen et al 2012).

One might ask why we do not observe any link between gas-rich central galaxies of low stellar masses and blue/star-forming neighbours. This might be expected in a scenario in which star formation in low mass galaxies is fuelled by accretion of cold gas from surrounding filaments. However, as we have discussed, the dominant source of gas infall at low redshifts may be in the form of material previously ejected by supernovae-driven winds (see also Oppenheimer et al 2010). The extent to which this gas would correlate with the present-day population of galaxies is currently not understood.

6.3 Implications for large-scale structure studies

We note that a large fraction of current work in cosmology is based on the premise that the statistical properties of a galaxy population can be predicted if one knows just two things: a) the mass distribution of the dark matter halos that host the galaxies, b) the location of the galaxies in their halos – in particular whether they are central galaxies or satellites. This forms the basis of the so-called halo occupation distribution (HOD) modelling technique. The HOD framework also lies at the root of the idea that galaxies trace the underlying distribution in a simple enough way that they can be used as cosmological probes with high precision.

Most analyses that have tested the halo model have used luminosity or stellar mass-selected samples as their basis. However, future Baryon Acoustic Oscillation experiments such as HETDEX and BigBOSS aim to work with high-redshift galaxies selected by their emission line properties. It is possible that the large-scale conformity effects discussed in this paper will affect clustering statistics in emission-line-selected galaxy surveys more than in stellar mass-selected galaxy surveys. In Figure 12, we show the me-

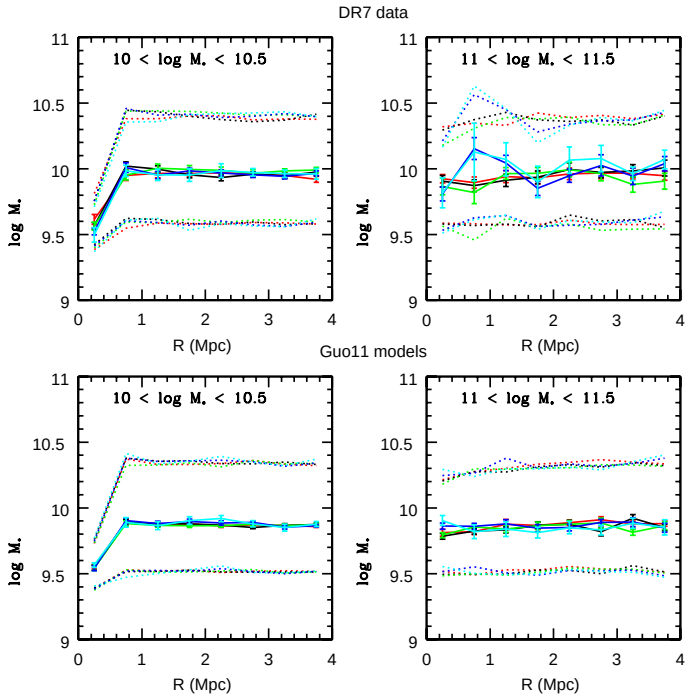

Figure 12. The median stellar masses of neighbouring galaxies (solid lines), as well as the 25th and 75th percentiles of the stellar mass distributions of these objects (dotted lines), are plotted as a function of projected distance from central galaxies in the model. Results are shown for central galaxies in two stellar mass ranges. The central galaxies have been ordered by cold gas mass fraction and colour-coded as in previous figures. Results from the SDSS DR7 are shown in the top two panels, while results from the Guo et al. (2011) models are shown in the bottom panels.

dian as well as the 25th and 75th pecentiles in the *stellar masses* of neighbouring galaxies as a function of projected radius from the central. As can be seen, there is *no conformity* between the gas fraction of centrals and the stellar masses of neighbours both in the data and in the models. As is already known (Guo et al 2011), the stellar mass distributions in the data and the models agree very well.

Finally, we would like to note that it would be useful to search for direct evidence of pre-heating of the gas around red, low mass galaxies using quasar absorption lines as probes of the temperature of the surrounding IGM. It will also be important to understand the physical processes responsible for the heating. The strong correlation between gas content in low mass central galaxies and the timescale over which the neighbouring galaxies are building their *central* stellar populations offers a tantalizing hint that feedback processes associated with galaxy bulge and black hole formation may play a role. This will be the subject of future work.

ACKNOWLEDGMENTS

Thank you to the Aspen Center for Physics and the NSF Grant No. 1066293 for hospitality, support and peace-of-mind during the conception and writing of this paper.

REFERENCES

Ann H. B., Park C., Choi Y.-Y., 2008, MNRAS, 389, 86
Baldry I. K., Balogh M. L., Bower R. G., Glazebrook K., Nichol R. C., Bamford S. P., Budavari T., 2006, MNRAS, 373, 469
Berlind A. A., Blanton M. R., Hogg D. W., Weinberg D. H., Davé R., Eisenstein D. J., Katz N., 2005, ApJ, 629, 625
Blanton M. R., et al., 2005, AJ, 129, 2562
Boylan-Kolchin M., Springel V., White S. D. M., Jenkins A., Lemson G., 2009, MNRAS, 398, 1150
Brinchmann J., Charlot S., White S. D. M., Tremonti C., Kauffmann G., Heckman T., Brinkmann J., 2004, MNRAS, 351, 1151
Catinella B., et al., 2010, MNRAS, 403, 683
Chen Y.-M., et al., 2012, arXiv, arXiv:1208.1584
Cole S., Aragon-Salamanca A., Frenk C. S., Navarro J. F., Zepf S. E., 1994, MNRAS, 271, 781
Croton D. J., et al., 2006, MNRAS, 365, 11
De Lucia G., Kauffmann G., White S. D. M., 2004, MNRAS, 349, 1101
Font A. S., et al., 2008, MNRAS, 389, 1619
Guo Q., et al., 2011, MNRAS, 413, 101
Heckman T. M., Kauffmann G., Brinchmann J., Charlot S., Tremonti C., White S. D. M., 2004, ApJ, 613, 109
Kauffmann G., White S. D. M., Guiderdoni B., 1993, MNRAS, 264, 201
Kauffmann G., Li C., Heckman T. M., 2010, MNRAS, 409, 491
Li C., Kauffmann G., Fu J., Wang J., Catinella B., Fabello S., Schiminovich D., Zhang W., 2012, MNRAS, 424, 1471
McKay T. A., et al., 2002, ApJ, 571, L85
Mo H. J., Mao S., 2002, MNRAS, 333, 768
Mo H. J., Yang X., van den Bosch F. C., Katz N., 2005, MNRAS, 363, 1155
More S., van den Bosch F. C., Cacciato M., Mo H. J., Yang X., Li R., 2009, MNRAS, 392, 801
Norberg P., Frenk C. S., Cole S., 2008, MNRAS, 383, 646
Oppenheimer B. D., Davé R., Kereš D., Fardal M., Katz N., Kollmeier J. A., Weinberg D. H., 2010, MNRAS, 406, 2325
Prada F., et al., 2003, ApJ, 598, 260
Sales L., Lambas D. G., 2004, MNRAS, 348, 1236
Sales L. V., Wang W., White S. D. M., Navarro J. F., 2012, arXiv, arXiv:1208.2027
Salim S., et al., 2007, ApJS, 173, 267
Schlegel D. J., Finkbeiner D. P., Davis M., 1998, ApJ, 500, 525
Valageas P., Silk J., 1999, A&A, 350, 725
Wang Y., Yang X., Mo H. J., van den Bosch F. C., Katz N., Pasquali A., McIntosh D. H., Weinmann S. M., 2009, ApJ, 697, 247
Wang W., White S. D. M., 2012, MNRAS, 424, 2574
Weinmann S. M., van den Bosch F. C., Yang X., Mo H. J., 2006, MNRAS, 366, 2
Weinmann S. M., Kauffmann G., von der Linden A., De Lucia G., 2010, MNRAS, 406, 2249
Wyder T. K., et al., 2007, ApJS, 173, 293
Yang X., Mo H. J., van den Bosch F. C., Jing Y. P., 2005, MNRAS, 356, 1293
Yang X., Mo H. J., van den Bosch F. C., 2006, ApJ, 638, L55

Yang X., Mo H. J., van den Bosch F. C., 2008, ApJ, 676, 248
Zhang W., Li C., Kauffmann G., Xiao T., 2012, arXiv, arXiv:1207.3924